




Resilience, Dynamics, and Interactions within a Model Multispecies Exoelectrogenic-Biofilm Community

Anna Prokhorova,^a Katrin Sturm-Richter,^a  Andreas Doetsch,^b Johannes Gescher^{a,c}

Institute for Applied Biosciences, Department of Applied Biology, Karlsruhe Institute of Technology, Karlsruhe, Germany^a; Institute of Functional Interfaces, Department of Interface Microbiology, Karlsruhe Institute of Technology, Eggenstein-Leopoldshafen, Germany^b; Institute for Biological Interfaces, Karlsruhe Institute of Technology (KIT), Eggenstein-Leopoldshafen, Germany^c

ABSTRACT Anode-associated multispecies exoelectrogenic biofilms are essential for the function of bioelectrochemical systems (BESs). The individual activities of anode-associated organisms and physiological responses resulting from coculturing are often hard to assess due to the high microbial diversity in these systems. Therefore, we developed a model multispecies biofilm comprising three exoelectrogenic proteobacteria, *Shewanella oneidensis*, *Geobacter sulfurreducens*, and *Geobacter metallireducens*, with the aim to study in detail the biofilm formation dynamics, the interactions between the organisms, and the overall activity of an exoelectrogenic biofilm as a consequence of the applied anode potential. The experiments revealed that the organisms build a stable biofilm on an electrode surface that is rather resilient to changes in the redox potential of the anode. The community operated at maximum electron transfer rates at electrode potentials that were higher than 0.04 V versus a normal hydrogen electrode. Current densities decreased gradually with lower potentials and reached half-maximal values at -0.08 V. Transcriptomic results point toward a positive interaction among the individual strains. *S. oneidensis* and *G. sulfurreducens* upregulated their central metabolisms as a response to cultivation under mixed-species conditions. *G. sulfurreducens* was detected in the planktonic phase of the bioelectrochemical reactors in mixed-culture experiments but not when it was grown in the absence of the other two organisms.

IMPORTANCE In many cases, multispecies communities can convert organic substrates into electric power more efficiently than axenic cultures, a phenomenon that remains unresolved. In this study, we aimed to elucidate the potential mutual effects of multispecies communities in bioelectrochemical systems to understand how microbes interact in the coculture anodic network and to improve the community's conversion efficiency for organic substrates into electrical energy. The results reveal positive interactions that might lead to accelerated electron transfer in mixed-species anode communities. The observations made within this model biofilm might be applicable to a variety of nonaxenic systems in the field.

KEYWORDS bioelectrochemical systems, *Shewanella*, *Geobacter*, exoelectrogenic biofilm, transcriptome analysis

Several microorganisms have the ability to transfer respiratory electrons to an extracellular electron acceptor. Extracellular respiration is highly relevant for a number of biogeochemical cycles, because these electron transport chains were developed for reducing metal oxides as well as for nonmembrane-permeable environmental electron shuttles, such as humic substances (1–4). It is likely that the selective pressure to evolve terminal reductases that catalyze electron transfer to solid electron

Received 2 November 2016 Accepted 2 January 2017

Accepted manuscript posted online 13 January 2017

Citation Prokhorova A, Sturm-Richter K, Doetsch A, Gescher J. 2017. Resilience, dynamics, and interactions within a model multispecies exoelectrogenic-biofilm community. *Appl Environ Microbiol* 83:e03033-16. <https://doi.org/10.1128/AEM.03033-16>.

Editor Hideaki Nojiri, University of Tokyo

Copyright © 2017 American Society for Microbiology. All Rights Reserved.

Address correspondence to Johannes Gescher, johannes.gescher@kit.edu.

acceptors forced the microorganisms to develop rather unspecific enzymes. These enzymes can catalyze the transfer of electrons to a variety of surfaces and substances that are characterized basically by a redox potential higher than -200 mV versus a normal hydrogen electrode (5). This lack of specificity enables the application of these microorganisms in so-called bioelectrochemical systems (BESs), in which they catalyze direct or indirect electron transfer to electrode surfaces (6–8). Recently, many studies were carried out to expand the application of BESs and increase the efficiency of electricity production (9–11). One strategy is to understand and steer the microbial community on electrode surfaces (12). We are far from understanding the role of individual groups of microorganisms that thrive on anode surfaces in nonaxenic systems. The interactions are most likely as diverse as they are in natural environments, in which, for instance, syntrophic associations between microorganisms play a dominant role in the overall fitness of the communities (13–15). The positive effect from coculturing in bioelectrochemical systems was already studied with synthetic communities (16–18). Nevertheless, an in-depth molecular analysis of biofilm interactions between organisms that must share the anode as a terminal electron acceptor has not yet been conducted.

To date, several exoelectrogenic bacteria have been identified. The predominant model organisms studied belong to the *Geobacteraceae* and *Shewanellaceae* families (19). Even with these model organisms, an understanding of the performance of electrochemically active coculture biofilms remains poor due to the limited knowledge of possible microbial interactions between these organisms. The respiratory activity of microbial communities on anodes can be monitored as current generation, and the anode potential can be controlled by a potentiostat (20) that enables acceleration or suppression of extracellular electron transfer rates in the biofilm community as a function of the applied surface redox potential (21, 22). It is still poorly understood how the electrode potentials affect the developmental processes in an exoelectrogenic community and how metabolic networks are established and maintained within the community.

To determine whether exoelectrogenic organisms show distinct responses as a consequence of coculturing and to analyze the stability of these anode-associated biofilms under different applied potentials that will lead to different respiratory activities, it is necessary to develop a biofilm composed of exoelectrogenic model organisms. The proteobacteria *Shewanella oneidensis* MR-1, *Geobacter sulfurreducens* PCA, and *Geobacter metallireducens* GS-15 are well studied and have different characteristics that *per se* enable stable coculturing. *S. oneidensis* is a facultative anaerobic organism. It has a rather narrow spectrum of usable electron donors and shows only partial oxidation of the used carbon and electron sources to a mixture of acetate, formate, CO_2 , and hydrogen as end products of its anaerobic metabolism (23, 24). Lactate seems to be the preferred electron donor under anoxic conditions (23). Several studies have found that *S. oneidensis* releases flavin molecules that can be used as endogenous electron shuttles under batch culture conditions (25–27). Hence, the organism can grow planktonically while still interacting with the electron acceptor by the use of such shuttle molecules. *S. oneidensis* cells can also grow as a biofilm in direct contact with the electrode, but these biofilms are rather thin (28). *G. sulfurreducens* is the most-studied organism within *Geobacteraceae*. Several research groups characterized the strain in bioelectrochemical systems because it forms biofilms that are several micrometers thick and typically shows 5-fold higher current production than *S. oneidensis* (29). The organism uses acetate as the preferred carbon and electron sources and was classified as oxygen tolerant (30). Lin et al. reinvestigated its oxygen sensitivity in 2004 and demonstrated that *G. sulfurreducens* not only is oxygen tolerant but can even grow with oxygen as the sole electron acceptor if added in concentrations up to 10% to the headspace of the culture (31). *G. metallireducens* has an extremely wide spectrum of growth substrates, including propionate, acetate, and others. The organism is oxygen sensitive, and current production was shown to be similar to or slightly lower than that by *G. sulfurreducens* (32–34). Both *Geobacter* strains depend on short-range electron

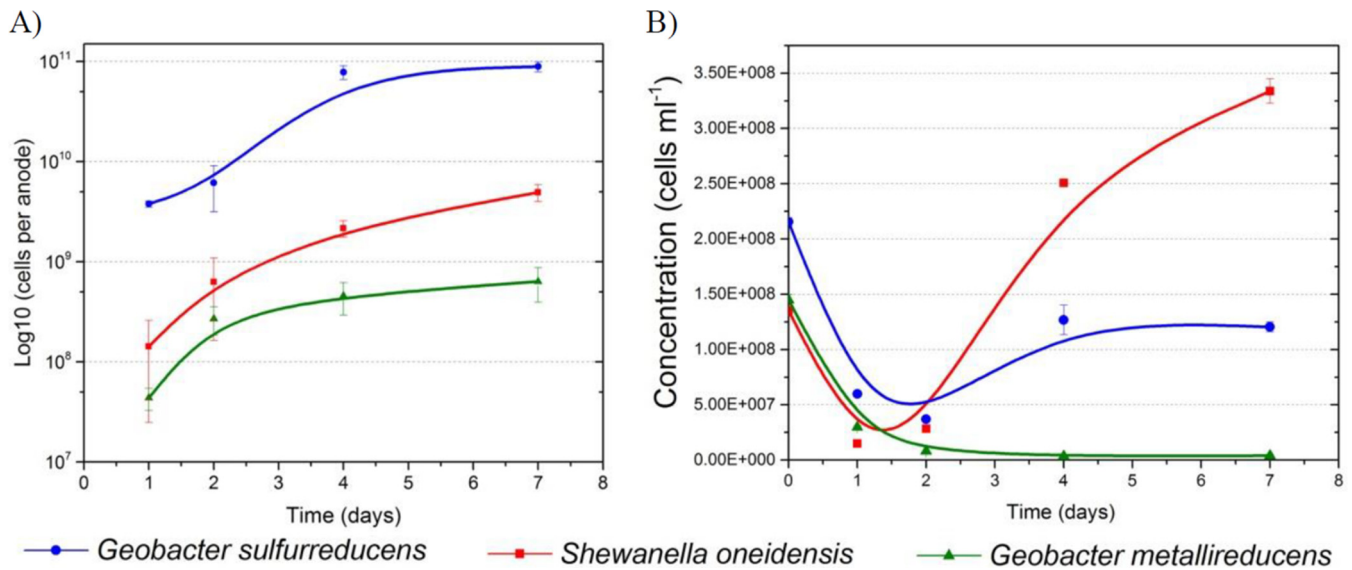


FIG 1 Growth of the model exoelectrogenic biofilm directly on the anode surface (left) and in the planktonic phase (right) over a time course of 7 days. The analyses were conducted at different time points following inoculation, with an initial inoculum that consisted of equal fractions of the three barcoded strains. Cell numbers were quantified using qPCR.

transfer via direct contact and/or long-range electron transfer via conductive pili. For *Geobacteraceae*, the latter seems to be an important or even necessary feature for thick and highly conductive biofilms and for participation in direct interspecies electron transfer (DIET), since *G. uraniireducens*, a strain that produces pili with low conductivity, cannot participate in DIET and produces thin and poorly conductive biofilms (35).

In this study, we developed an anode-associated biofilm composed of the three model organisms and studied the dynamics of biofilm formation and the stability at different applied anode potentials. The physiological role of the three model organisms and their potential interactions were analyzed with a (meta-)transcriptomic approach. Our analysis highlights the different ecological niches of the three model organisms that enable not only parallel growth but also a positive interaction.

RESULTS AND DISCUSSION

Dynamics of a model multispecies anode biofilm formation. The overall aims of this study were to analyze the dynamics of community composition and metabolic processes of a controlled microbial community on anode surfaces, as well as to try to unravel the possible mutual effects within the biofilm community. In the first set of experiments, the dynamics of a biofilm composed of the three model organisms, *S. oneidensis*, *G. sulfurreducens*, and *G. metallireducens*, was analyzed over a time course of 7 days. The three strains were added with optical density (OD) values equal to those of the microbial electrochemical cells so that the final optical density was 0.1. The OD values from similar cell numbers of different species did not correspond due to the differences in cell size among these strains. The anode potential was adjusted to 0 mV. The compositions of anode biofilms, as well as the planktonic community, were analyzed in triplicate 1, 2, 4, and 7 days following inoculation, using quantitative PCR (qPCR). *G. sulfurreducens* clearly dominated the sessile community beginning on the first day (Fig. 1A). This was expected, as the strategy of *G. sulfurreducens* cells for electron transfer to insoluble electron acceptors relies solely on a direct interaction that is mediated by conductive pili and *c*-type cytochromes on the surfaces of the cells and within the extracellular matrix (25). Nevertheless, neither *S. oneidensis* nor *G. metallireducens* was outcompeted from the anode during the time course of the experiment. On the contrary, we observed active growth. Results from the planktonic phase (Fig. 1B) revealed a more dynamic development of the community than in the anode biofilm. The percentage of *S. oneidensis* cells increased within the first 4 days to 73%, while *G.*

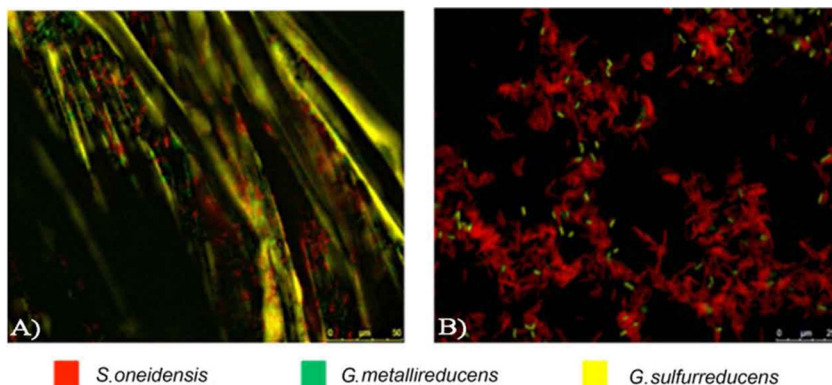


FIG 2 Fluorescent *in situ* hybridization (FISH) in the exoelectrogenic community. Shown are cells on the anode surface (A) and cells in the planktonic phase (B) after 7 days of the experiment. *G. sulfurreducens* is in yellow (Cy5), *G. metallireducens* is in green (fluorescein isothiocyanate [FITC]), and *S. oneidensis* is in red (Cy3).

metallireducens cells were almost eliminated from the planktonic phase. This might be due to oxygen contamination within the reactor, as will be stated in later parts of this report. *G. sulfurreducens* cells accounted for 27% of the overall community. The flavin concentration in the medium increased slightly but significantly (1.34-fold) to 37.5 nM ($P = 0.023$, unpaired *t* test, heteroscedastic) compared with that at the start of the experiments. Unexpectedly, for an unknown reason, the flavin concentration decreased when the same experiment was conducted with either one of the three individual strains alone (see Fig. S1 in the supplemental material). Hence, it is possible that flavins were used as mediators for electron transfer by the two strains found in the planktonic phase of the coculture reactors.

Results from fluorescent *in situ* hybridization (FISH) experiments corroborated the qPCR-based results (Fig. 2). The micrographs also displayed the different sizes of *Shewanella* compared with those of *Geobacter* cells that result in starting compositions of equal OD values but different concentrations of the individual strains. After 2 to 3 days of cultivation, the multispecies biofilm generated stable currents that reached values between 0.60 to 0.64 mA/cm². This observation indicates that the community within the BESs achieved stable rates of carbon oxidation.

Characterization of the biofilm stability under different electrochemical conditions. In the second set of experiments, the stability of the previously described multispecies biofilm was investigated under various electrochemical process parameters. Fifteen BES reactors were started at the same time under the following applied potentials: 0.44 V, 0.24 V, 0.04 V, -0.06 V, and -0.16 V. Interestingly, the current values produced were highly similar during the time course of the experiment, when the applied potential was in a range between 0.04 and 0.44 V (Fig. 3). Lower currents were observed only if the working electrodes were poised to potentials lower than 0.04 V.

The biofilm community compositions at the completion of the experiments were similar under each of the tested conditions and were comparable to the results shown in the previous section (Fig. 4). At the end of the 7 days of incubation, *G. sulfurreducens* accounted for 86% to 96% of all organisms. *S. oneidensis* cells represented 4% to 12% of the community, while *G. metallireducens* was only detectable in minor quantities. In line with the measured current densities, we saw a pronounced drop in cell density when potentials lower than 0 mV were applied. Working electrodes poised to a potential of -0.06 V had >80% fewer cells than anodes adjusted to a potential of 0.04 V. In comparison, all anodes poised to positive values showed only minor differences in terms of overall cell numbers. Planktonic cells in the reactors were also quantified. Here, *S. oneidensis* (57 to 73%) and *G. sulfurreducens* (26 to 43%) comprised the majority of organisms (Fig. 4). It seemed that working electrode potentials higher than -0.06 V sustained the maximum rate of electron transfer, which correlates to the highest

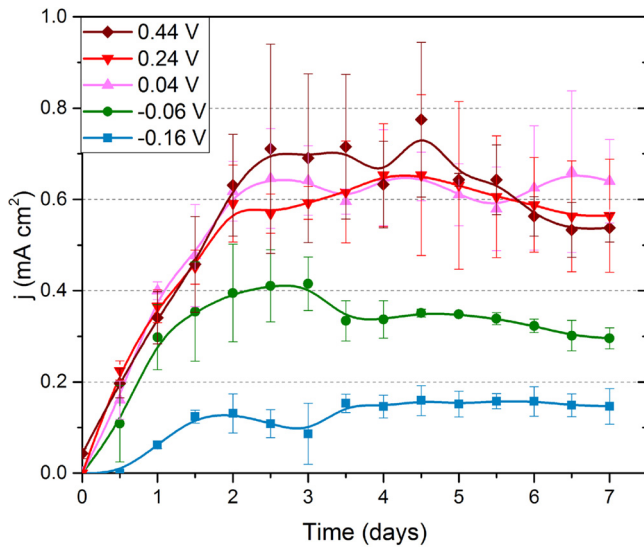


FIG 3 Stability of the model exoelectrogenic biofilm under different applied potentials (versus NHE). Under positive applied potentials (0.04 to 0.44 V), current densities (j) were roughly identical and were in the range of 0.5 to 0.7 mA cm⁻².

biomass production rates. While *S. oneidensis* and *G. sulfurreducens* responded similarly to the different potentials, we did not observe as clear of a trend for *G. metallireducens*. It is possible that under the chosen conditions, the growth of *G. metallireducens* was limited by the substrate oxidation rate rather than by electron transfer to the anode surface.

Steering metabolic activity via working electrode potentials. Linear sweep voltammetry was conducted to determine the minimal potential at which an exoelectrogenic multispecies biofilm transfers respiratory electrons to the working electrode. An initial applied potential of 0.04 V was linearly decreased to -0.26 V, with a sweep rate of 0.75 μV s⁻¹. Thereafter, the sweep was repeated in the reverse direction until the starting potential of 0.04 V was reached. As indicated in Fig. 5, the cells stopped producing current when the applied potential was lower than approximately -0.2 V.

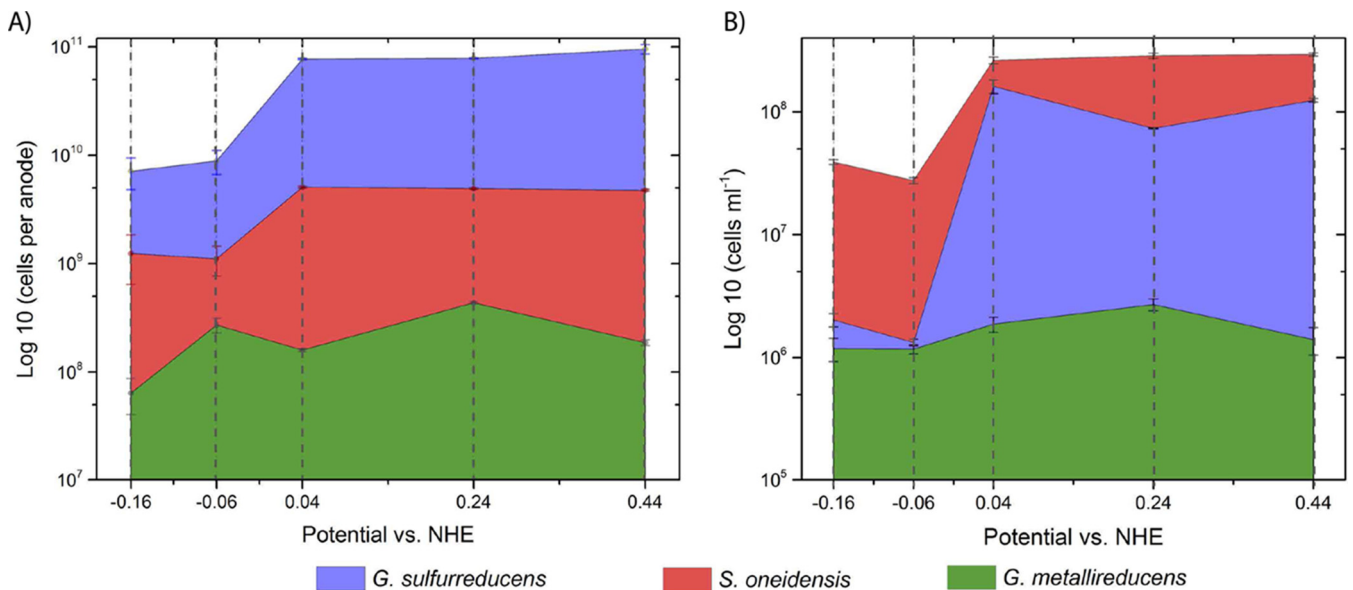


FIG 4 Quantitative analysis of the cells on the anode surface (A) and in the planktonic phase (B) under different applied potentials and after 7 days of growth in the bioelectrochemical reactor.

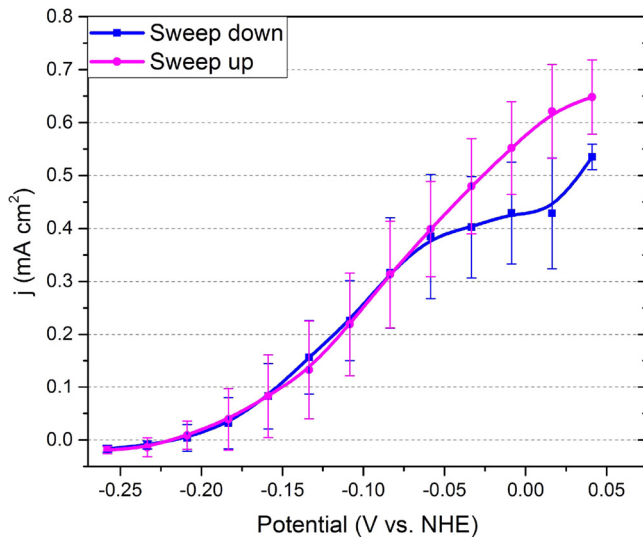


FIG 5 Stability and activity of the model exoelectrogenic biofilm during a linear sweep voltammetry experiment. The applied potentials ranged from 0.05 mV to -0.25 mV against NHE. The experiment was initiated at 0.05 mV. After reaching -0.25 mV, the sweep was reversed back to 0.05 mV. The limiting potential, at which cells stopped producing electrons, was detected at below approximately -0.2 V.

Half-maximal electron transfer rates were achieved with an anode potential of -0.08 V. This potential is in line with typical midpoint potentials of outer membrane cytochromes, as well as with flavins, which are released by *S. oneidensis* and can be used as electron transfer shuttles (27, 36, 37). Immediately after reaching -0.26 V, the experiment was repeated in the reverse potential direction. The current-over-potential diagram showed a very similar progression. The consortium stability did not seem to be highly affected by variations of electron transfer rates. This is surprising, since the very low sweep rate resulted in an overall time course for the experiment of more than 9 days for the complete sweep from 0.04 V down to -0.26 V and back up to 0.04 V. The ability to control current production by exoelectrogenic bacteria might offer promising solutions for applied processes.

Transcriptome analysis. Transcriptomes and metatranscriptomes were analyzed to reveal metabolic changes in the individual strains as a result of the shift from solitary to multispecies growth on anodes, thereby illuminating the observation that multispecies biofilms often produce higher current densities than axenic cultures. Twelve BES reactors were started. They contained, in triplicates, either single cultures of *S. oneidensis*, *G. sulfurreducens*, and *G. metallireducens* or a mixture of all three strains. The applied working electrode potential in all cases was 0.04 V. The experiment was conducted over a 7-day time period. From the second day onward, medium was continuously pumped through the reactors to reach a hydraulic retention time of 160 min. The medium contained lactate and propionate as carbon and electron sources. To provide concentrations of electron donors that were similar to those of the coculture experiments, acetate (5 mM) was added in the experiments that were conducted solely with *G. sulfurreducens*. Summers et al. (38) showed that wild-type *G. sulfurreducens* grows on lactate (this is contrary to the results in a publication by Caccavo et al. [30]). According to Summers et al., growth rates were very low and increased to 8 h only after a spontaneous point mutation. Under coculture conditions, acetate was produced by *S. oneidensis* as an end product of lactate oxidation.

The concentrations of the different carbon sources were assessed in the media after day 3, as the growth experiments revealed rather stable cell numbers in the second half of the experiment under coculture conditions (Fig. 6). *S. oneidensis* metabolized 8 mM lactate on average and produced 7 mM acetate. Interestingly, the growth of *S. oneidensis* led to the concomitant production of 3.8 mM propionate, which

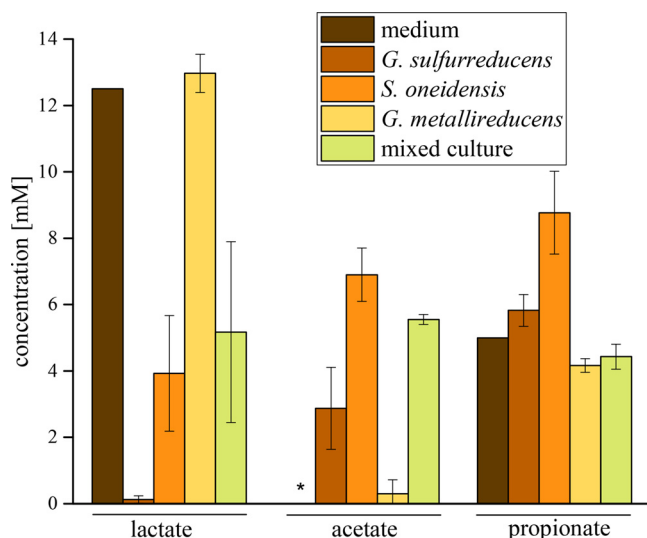


FIG 6 Organic acid concentrations in the media and the different BES reactors at day 3 (pumping period, stable cell numbers). Added to the media were 12.5 mM lactate, 0 mM acetate, and 5 mM propionate. Error bars represent the standard deviations from means of samples taken in independent triplicates. *, 5 mM acetate was added to the medium for the pure culture of *G. sulfurreducens* in the BES reactor.

most likely resulted from the consumption of amino acids from the medium. The latter was also corroborated by the results from the transcriptome analysis. Formate was not detected in the spent medium. In single cultures, *G. sulfurreducens* consumed 2.1 mM of the added 5 mM acetate on average. Lactate was not consumed, while the propionate concentration increased from 5 to 5.8 mM. *G. metallireducens* metabolized 0.8 mM propionate, while a decrease in lactate concentration was not detectable. In cocultures, we observed a decrease in the propionate concentration of 0.6 mM, while 7.3 mM lactate was consumed. The acetate concentration was 5.6 mM. Hence, the observed lactate consumption rate was very similar to that of the pure culture experiment with *S. oneidensis* alone. The available acetate concentration in the coculture experiment would be 6.6 mM if it is assumed that the same ratio of catabolic lactate consumption that was observed in the *S. oneidensis* single culture can be applied to the coculture experiment. Even though two *Geobacter* strains could potentially thrive using the produced acetate, the acetate consumption was lower than in the experiment with *G. sulfurreducens* alone. Regarding propionate consumption, it is hard to estimate to what extent *G. metallireducens* cells metabolize propionate in the coculture. The concentration was lower than the added 5 mM, but we cannot say to what extent *S. oneidensis* produces propionate under coculture conditions. Nevertheless, the expression levels of the genes involved in branched-chain amino acid metabolism were downregulated under coculture conditions in *S. oneidensis*.

The bioelectrochemical reactors that were used in this study were constructed from polycarbonate, which is not gas tight. Moreover, the cathode compartment was separated from the anode by a Fumapem membrane, which is a possible source of contaminating oxygen in the anode. Therefore, the oxygen concentrations in all bioelectrochemical reactors were measured at the completion of the individual experiments (see Fig. S2). Oxygen reached a concentration of 19.9 μM in the reactors operated with *G. metallireducens* alone. In contrast, when the reactors were operated with *S. oneidensis* alone, *G. sulfurreducens* alone, or the mixture of all three strains, the oxygen concentration reached values of 4.3, 4.2, and 4.8 μM , respectively (Fig. S2). Hence, it seems as if the abilities of *S. oneidensis* and *G. sulfurreducens* to thrive using oxygen as an electron acceptor led to a depletion of oxygen in the reactors. Interestingly, we detected *G. sulfurreducens* cells only under coculture conditions in the planktonic phase. As the oxygen concentrations were similar when *G. sulfurreducens*

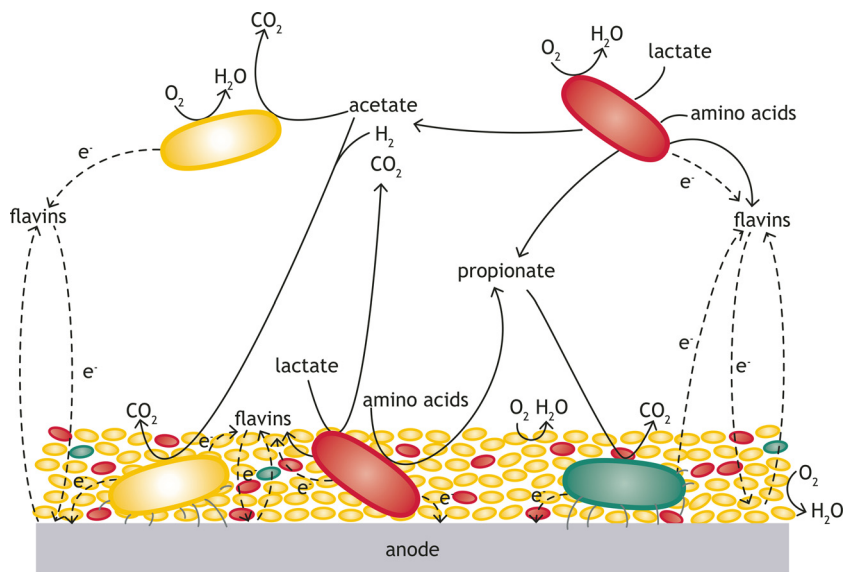


FIG 7 Proposed microbe-microbe and microbe-electrode interactions in the model multispecies biofilm. *S. oneidensis* uses lactate as an electron donor and produces acetate along with hydrogen and carbon dioxide. Acetate and hydrogen are consumed by *G. sulfurreducens* as electron donors. *G. metallireducens* is proposed to consume propionate as the primary electron donor. While *G. sulfurreducens* and *G. metallireducens* transfer electrons via direct contact with the electrode or by using nanowires (illustrated by gray lines), *S. oneidensis* can use flavin molecules as electron shuttles. It is also possible that the *Geobacter* strains use flavins released by *S. oneidensis* cells as electron shuttles in the planktonic phase of the reactor. Moreover, *S. oneidensis* and *G. sulfurreducens* protect *G. metallireducens* from oxidative stress by reducing oxygen to water. *G. sulfurreducens* cells are yellow in color, *S. oneidensis* cells are red, and *Geobacter metallireducens* are green. Metabolic exchange reactions between the organisms are represented by continuous arrows; electron transfer reactions are represented by dotted arrows.

was grown alone or together with *S. oneidensis* and *G. metallireducens*, it is unlikely that the toxic effects due to reactive oxygen species were the only reason that planktonic cells of *G. sulfurreducens* were observed only under coculture conditions. The higher flavin concentrations measured in the coculture experiment might lead to more pronounced electron shuttling via this mediator and might enable the growth of *G. sulfurreducens* in the planktonic phase, but this needs to be investigated in further studies.

During solitary growth, each of the strains produced less current than that from coculture conditions (0.62 mA cm^{-2}). The highest current production in solitary growth was recorded for *G. sulfurreducens* (0.47 mA cm^{-2}), whereas *S. oneidensis* produced only around 0.13 mA cm^{-2} and *G. metallireducens* produced 0.06 mA cm^{-2} .

A comparison of the transcriptomes from solitary and coculture growths revealed that 1,124 of the 3,430 protein-coding genes of *G. sulfurreducens* showed log₂-fold changes higher than ± 1 with corresponding adjusted *P* values (*P* adj) of less than 0.05. Of the total 4,214 genes of *S. oneidensis*, 677 followed the above-described characteristics, while in *G. metallireducens*, only 23 genes were detected as differentially expressed (see Table S1). This rather low number of detectable candidate genes might be due to a reduced experimental sensitivity caused by limited growth of the *G. metallireducens* cells compared with the other two strains and its subsequently reduced representation in the coculture transcriptomic data.

Variations of the central metabolism as a result of cocultivation. As mentioned above, a multitude of genes were differentially expressed between cells grown in the absence or presence of other organisms that thrive on the anode surface. This study focused on the central metabolic changes that result from cocultivation of the strains. The data presented suggest a number of interactions that are summarized in Fig. 7.

Geobacter sulfurreducens. Generally, it seems as if the central metabolism of *G. sulfurreducens* is upregulated under coculture conditions (Table 1).

TABLE 1 Differential expression of selected genes under coculture conditions with significantly altered transcription and discussed in this work

Species	Identifier	Gene	Function	Fold change ^a	Adjusted P
<i>G. sulfurreducens</i>	Upregulated				
	GSU2737	<i>omcB</i>	Outer membrane cytochrome	2.260	0.000
	GSU2731	<i>omcC</i>	Outer membrane cytochrome	3.656	0.000
	GSU0618	<i>omcE</i>	Outer membrane cytochrome	3.325	0.000
	GSU0612/GSU1024	<i>ppcA/D</i>	Periplasmic cytochrome	8.944 ± 1.280	0.000 ± 0.000
	GSU0466	<i>macA</i>	Cytochrome c peroxidase	6.591	0.000
	GSU2739	<i>ombB</i>	Beta barrel porin	3.551	0.111
	GSU2733	<i>ombC</i>	Beta barrel porin	2.794	0.102
	GSU2449/48/1059	<i>sucABD</i>	Succinate dehydrogenase	5.256 ± 1.744	0.000 ± 0.000
	GSU1177/8	<i>frdA/B</i>	Fumarate reductase	2.288 ± 1.032	0.000 ± 0.000
	GSU0994	<i>fumB</i>	Fumarate hydratase	2.029	0.001
	GSU1106	<i>glTA</i>	Citrate synthase	2.016	0.001
	GSU2445	<i>acn</i>	Aconitate hydratase	7.885	0.000
	GSU3628	<i>pgk</i>	Phosphoglycerate kinase	2.469	0.000
	GSU0490	<i>atoA</i>	Succinyl:acetate coenzyme A transferase	2.401	0.000
	GSU3331	<i>pyk</i>	Pyruvate kinase	1.516	0.086
	GSU2286	<i>eno</i>	Enolase	2.44	0.000
	GSU1496	<i>pilA</i>	Pilin	2.61	0.000
	GSU2011	<i>nifS</i>	Nitrogen fixation protein	2.539	0.000
	GSU0782–87	<i>hyb</i> cluster	Hydrogenase	17.533 ± 2.407	0.000 ± 0.000
	GSU3429–44	<i>nuo</i> cluster	NADH dehydrogenase	2.876 ± 1.272	0.014 ± 0.019
	GSU2352	<i>aplC</i>	Acetate symporter	4.816	0.042
	Downregulated				
GSU1640/1	<i>cydA/B</i>	Cytochrome <i>bd</i> menaquinol oxidase	−5.760 ± 1.087	0.000 ± 0.000	
GSU3364	<i>hgtR</i>	Hydrogen-dependent growth transcriptional repressor	−6.325	0.000	
<i>S. oneidensis</i>	Upregulated				
	SO_1776	<i>mtrB</i>	Beta barrel protein	2.086	0.013
	SO_1777	<i>mtrA</i>	Periplasmic cytochrome	2.190	0.031
	SO_1778	<i>mtrC</i>	Outer membrane cytochrome	2.548	0.002
	SO_1779	<i>omcA</i>	Outer membrane cytochrome	2.289	0.012
	SO_1518–22	<i>lld</i> cluster	L-Lactate dehydrogenase	4.135 ± 1.395	0.011 ± 0.013
	SO_2090/3/4	<i>hypBEF</i>	Hydrogenase	3.171 ± 1.329	0.009 ± 0.013
	SO_2095–9	<i>hyaABCDE</i>	Hydrogenase	6.552 ± 1.468	0.000 ± 0.001
	SO_2912/3	<i>pflB/A</i>	Pyruvate formate lyase	2.934 ± 1.050	0.011 ± 0.005
	SO_4509/10/11	<i>fdhABC</i>	Formate dehydrogenase	3.563 ± 1.056	0.000 ± 0.000
	Downregulated				
	SO_1891–98	<i>liu</i> cluster	Amino acid degradation	−8.944 ± 1.342	0.000 ± 0.000
	SO_1677–82	<i>ivd</i> cluster	Amino acid degradation	−6.307 ± 1.301	0.000 ± 0.000
SO_0342/44/45/46/1900	<i>prpF/C/B/R/E</i>	Propionate oxidation	−4.305 ± 1.499	0.000 ± 0.002	
<i>G. metallireducens</i>	Upregulated				
	Gmet_1122	<i>prpB</i>	2-Methylisocitrate lyase	1.341	0.000
	Gmet_1123	<i>prpD</i>	2-Methylcitrate dehydratase	1.786	0.009
	Downregulated				
	Gmet_1929	<i>cydB</i>	Cytochrome <i>bd</i> menaquinol oxidase, subunit II	−1.762	0.050
Gmet_1930	<i>cydA</i>	Cytochrome <i>bd</i> menaquinol oxidase, subunit I	−2.209	0.000	

^aMeans and standard deviations for fold changes in expression of clusters of genes in anodic cells in coculture/anodic cells in pure culture.

Outer membrane cytochromes, components of the membrane-spanning porin-cytochrome complex that transfer electrons across the outer membrane, several periplasmic and inner membrane-associated cytochromes, and the major pilus component *pilA* are upregulated under coculture conditions (Table 1). This indicates a generally more active transfer of electrons to the anode by *G. sulfurreducens* cells within the mixed species biofilm. Detailed information about the upregulated cytochromes and pilus genes can be found in the supplemental material. The hypothesis that increased electron transfer results from cocultivation is corroborated by the upregulation of genes coding for central reactions involved in the uptake (*atoA*) and oxidation of acetate via the citric acid cycle, as well for the NADH dehydrogenase, Nuo (Table 1; average upregulation of *nuo* genes, 2.9-fold). The reason for this general response might be that the hydrogen-dependent growth transcriptional regulator HgtR is down-

regulated. HgtR has been shown to repress genes involved in biosynthesis and energy generation (39). Although HgtR is downregulated under cocultivation conditions, the typical uptake hydrogenase, HybAB (40), of *G. sulfurreducens* is strongly upregulated (average upregulation of *hyb* genes, 17.5-fold). One explanation is that *G. sulfurreducens* under coculture conditions may enter a state in which it uses hydrogen (presumably provided by *S. oneidensis*; see below) and acetate as electron donors, whereas in pure cultures, acetate is the main carbon source. The use of hydrogen might also enable a higher proportion of acetate to be utilized in gluconeogenesis. At least two genes of gluconeogenesis were discovered to be upregulated under coculture conditions, namely, *eno* (2.4-fold upregulation) and *pgk* (2.5-fold upregulation). Interestingly, the results from the analysis of acetate concentrations in the coculture experiment suggest a lower acetate consumption rate than in the experiment with *G. sulfurreducens* alone. This result might corroborate the hypothesis of an increased usage of hydrogen as an electron and energy source. The transcription levels of genes necessary for nitrogen fixation strongly decreased as a result of cocultivation. This might indicate that, although the medium contains 3.7 mM ammonium, the cells encounter a nitrogen limitation within the anode biofilm in pure culture. Both *Geobacter* strains showed downregulations of *cydA* and *cydB* as a result of cocultivation. These encode cytochrome *bd* ubiquinol oxidase, which was discussed as a mechanism for coping with oxidative stress (41). The downregulation might be explained by the reduced respiration from the 20 μ M oxygen available in the anode chamber under cocultivation conditions shared by *S. oneidensis* and *G. sulfurreducens*.

***Geobacter metallireducens*.** In addition to the downregulation of genes involved with oxidative stress, *G. metallireducens* showed another adaptation to growth with *G. sulfurreducens* and *S. oneidensis*, namely, an upregulation of the *prp* operon (Table 1). The *prp* genes encode the proteins necessary for propionate oxidation (42). *G. metallireducens* can grow with acetate and propionate. These cells apparently do not adapt their metabolism for acetate as a carbon source but rather specialize in using propionate, for which there is no competitor in the community. Propionate is a challenging substrate under anoxic conditions, since its oxidation involves an energy-dependent activation to propionyl-CoA and an ATP-dependent oxidation of succinate to fumarate if electron acceptors are used, a reduction that is menaquinone dependent. This might also explain the rather low growth rate of *G. metallireducens* (43).

We observed that *S. oneidensis* cells grown alone in the anode medium produced propionate. Although the results from the transcriptomic analysis of the *S. oneidensis* cells (see below) predict that propionate production will be lower in the coculture experiment, it is possible that propionate produced by *S. oneidensis* is directly transferred to *G. metallireducens* within the anode biofilm. Propionate has antimicrobial activity. The mechanism through which it exerts this activity involves the uncoupling of the cytoplasmic membrane potential as it enters the cell as a protonated molecule and then its dissociation in the cytoplasm (44). Other lines of evidence suggest that the intracellular accumulation of volatile fatty acids like propionate blocks a number of metabolic pathways and consequently arrests cell growth (45). The parallel production and consumption of propionate by *S. oneidensis* and *G. metallireducens*, respectively, might lead to an overall fitness benefit for the biofilm by reducing the concentration of this antimicrobial compound.

***Shewanella oneidensis*.** *S. oneidensis* cells also showed distinct responses to growth in a coculture biofilm (Table 1). We observed an upregulation of the Mtr pathway, which is necessary for the transport of electrons through the outer membrane to an extracellular electron acceptor (*mtrABC* and *omcA* showed 2.3-fold upregulation on average). Furthermore, protein-coding genes involved in lactate transport and oxidation were also upregulated (SO_1518 to SO_1522; >4-fold). As was observed for *G. sulfurreducens*, cocultivation seemed to positively affect the substrate oxidation and electron transfer processes. It is possible that oxygen contamination in the reactors played a role. Although the oxygen concentrations in the reactors with *S. oneidensis*

alone or under coculture conditions were similar, oxygen was depleted simultaneously by *G. sulfurreducens* and *S. oneidensis* in the coculture experiment. *S. oneidensis* also responded to cocultivation by upregulating a hydrogenase (*hypBEF*, >3-fold; *hyaABCD*, >6-fold; see the supplemental material for further information). It was reported that hydrogen formation in *S. oneidensis* occurs under anoxic conditions in the absence of an electron acceptor and that hydrogen may be derived directly from pyruvate or indirectly from formate as the intermediate (46).

There are a number of gene clusters that were upregulated in cells grown in the absence of *G. sulfurreducens* and *G. metallireducens*. Very prominent were genes that are involved in degrading amino acids (the *liu* and *ivd* gene clusters). The medium contained Casitone and was therefore a source of amino acids. The catabolic consumption of amino acids, such as valine and isoleucine, by the *Ivd* proteins is corroborated by the observed production of propionic acid in the pure-culture experiment (47). Currently, we can only speculate that this distinct regulatory response was due to the faster depletion of the pool of available amino acids when the three organisms thrived simultaneously in the same reactor.

Conclusions. In this study, the interaction of three exoelectrogenic strains within BESs was analyzed. The biofilms formed on the anode surface appeared to be highly stable against fluctuations of the anode potential, which steered their respiratory activity. Although *G. metallireducens* plays a minor role in terms of cell size, it appears to occupy a stable ecological niche, which is likely characterized by the organism's ability to use propionate as an electron donor. *S. oneidensis* and *G. sulfurreducens* alone and together decreased the oxygen contamination in the reactor down to roughly 5 μM . This might positively affect the metabolism of the *G. metallireducens* biofilm. A transcriptomic analysis revealed that the interaction with other exoelectrogenic strains generally led to an upregulation in the expression of genes involved in the central metabolisms of the organisms, thus supporting the hypothesis of a positive interaction. The interaction between *G. sulfurreducens* and *S. oneidensis* is, for instance, likely displayed by the presence of a hydrogen cycle with *S. oneidensis* as a producer and *G. sulfurreducens* as a consumer. *G. sulfurreducens* cells were observed in the planktonic phase only in the presence of *S. oneidensis*. Further experiments are needed to reveal whether this was due to the use of flavins as electron shuttles by *G. sulfurreducens* cells. This would be similar to cheater-like behavior, as was described for extracellular signals in quorum-sensing studies (48, 49). The results presented in this report at least partially explain the observation reported multiple times in the literature that multispecies biofilms tend to be more efficient in current production than single cultures.

MATERIALS AND METHODS

Chemicals and biochemicals were obtained from Applichem (Darmstadt, Germany), Carl Roth GmbH & Co. KG (Karlsruhe, Germany), Sigma-Aldrich (Munich, Germany), Bioline (Luckenwalde, Germany), New England BioLabs (Frankfurt am Main, Germany), Fluka Chemie GmbH (Steinheim, Germany), and Thermo Scientific (Karlsruhe, Germany).

Bacterial strains and growth conditions. *S. oneidensis*, *G. sulfurreducens*, and *G. metallireducens* were routinely cultured anaerobically at 30°C in medium that was developed according to Coppi et al. (50) and Holmes et al. (51). The growth medium contained 0.42 g/liter KH_2PO_4 , 0.22 g/liter K_2HPO_4 , 0.2 g/liter NH_4Cl , 0.38 g/liter KCl, 0.36 g/liter NaCl, 0.21 g/liter $\text{MgCl}_2 \cdot 6\text{H}_2\text{O}$, 1.8 g/liter NaHCO_3 , 0.5 g/liter Na_2CO_3 , 60 mg/liter $\text{CaCl}_2 \cdot 2\text{H}_2\text{O}$, and 2 g/liter Casitone and was further complemented with 1.0 ml/liter selenite-tungstate solution (0.5 g/liter NaOH, 3 mg/liter Na_2SeO_3 , 4 mg/liter $\text{Na}_2\text{WO}_4 \cdot 2\text{H}_2\text{O}$), 10 ml/liter NB trace mineral solution (15, 50), 10 ml/liter vitamin solution (medium 141; German Type Culture Collection, DSMZ), 0.2 mM sodium ascorbate, 1.0 mM cysteine, 0.2% (wt/vol) yeast extract, and 50 mM ferric citrate as an electron acceptor. Although cysteine could theoretically act as a shuttling component, Straub and Schink indicated that it serves as a reducing agent rather than as an electron shuttle for *Geobacter* strains (52). The medium contained sodium lactate (12.5 mM), sodium acetate (6.25 mM), and sodium propionate (5 mM) as electron donors. These concentrations were chosen to enable electron acceptor limitation of the system. Standard anaerobic techniques were used throughout the study (53).

All anaerobic media were prepared in bottles capped with butyl rubber stoppers. To remove oxygen, the media were boiled for 10 min and flushed with a mixture of 80% N_2 :20% CO_2 for 30 min. The pH was then adjusted to 7.2. The optical density during anaerobic growth on ferric citrate was measured at a wavelength of 655 nm (OD_{655}) to avoid an influence by ferric iron. All experiments were carried out in at least three independent replicates. Error bars represent the standard deviations.

TABLE 2 Sequences of primers for qPCR^a

Probe name	Sequence (5' to 3')	Amplicon size (bp)
<i>S. oneidensis</i> for	GACTGTA CTGGCATTGG	18
<i>S. oneidensis</i> rev	GATCCATTAGCACAGACTTA	20
<i>G. sulfurreducens</i> for	CGGTTCTATCGACCTACC	18
<i>G. sulfurreducens</i> rev	CTGCTTGATGAACGAGAG	18
<i>G. metallireducens</i> for	CCGTGCTCTGTATGATAC	18
<i>G. metallireducens</i> rev	CAGGATTCTCGAATTCTC	20

^aSequences are from reference 55.

Preparation and operation of BES. The electrochemical reactors used in this study were described by Klope et al. (54). All experiments were carried out in a three-electrode setup. The individual chambers of the bioelectrochemical system (BES) were separated from each other by a Fumapem F-950 membrane (Quintech, Göppingen, Germany). A saturated calomel electrode (Sensortechnik Meinsberg GmbH, Ziegra-Knobelsdorf, Germany) was used as the reference electrode. Throughout the study, all potentials were corrected for the corresponding values against a normal hydrogen electrode (NHE). Two 2.25-cm² pieces of activated carbon cloth (C-Tex 13; MAST Carbon International, Ltd., Hampshire, United Kingdom) were used as an anode and cathode. The electrodes were connected to a potentiostat (Pine Instruments, Grove City, USA) using a titanium wire. All BES experiments were carried out at 30°C.

The medium for these experiments was composed as described above but did not contain a soluble electron acceptor. It contained 12.5 mM sodium lactate and 5 mM sodium propionate as electron donors. If *G. sulfurreducens* was cultured alone, 5 mM sodium acetate was added to the medium, since this strain cannot grow with propionate and only grows at a slow rate with lactate. In contrast, acetate is produced from lactate by *S. oneidensis*, which provides a constant acetate feed under coculture conditions. In all experiments, the anode chamber contained 22.5 ml of growth medium whereas the cathode chamber and the reference electrode compartment contained 25 ml and 5 ml, respectively, of medium without an electron donor or acceptor. Throughout the entire experiment, the anode chamber was flushed with a gas mixture of 80% N₂:20% CO₂ while an aerobic cathode served as a counter electrode.

Prior to all BES experiments, the cells were washed twice in a buffer containing 0.42 g/liter KH₂PO₄, 0.22 g/liter K₂HPO₄, 0.2 g/liter NH₄Cl, and 0.38 g/liter KCl, and then resuspended to an OD₆₅₅ of 1.0 in the same buffer. The initial cell densities in the BESs were set to an OD₆₅₅ of 0.1. The anode chamber was connected to a peristaltic pump, and after the first 24 h of the experiment, fresh medium was constantly pumped through the system at flow rate of 0.14 ml/min, resulting in a hydraulic retention time of 160 min.

Extraction and quantification of genomic DNA. Genomic DNA was extracted from the planktonic cells and the anode biofilm using the innuPREP stool DNA kit (Analytic Jena, Jena, Germany). Planktonic cells were treated as suggested by the manufacturer, while biofilm samples were additionally incubated in the lysis solution at room temperature for 10 min. Cell quantities were obtained by using quantitative PCR (qPCR) with primers specific for inserted barcode regions in the genome (Table 2 and reference 55). All experiments were conducted using independent biological triplicates and three technical replicates for each biological sample. To obtain the qPCR detection limits for each strain, a standard curve was constructed based on the threshold cycle (C_T) values for a dilution series of DNA from pure cultures (1, 1 × 10⁻¹, 2 × 10⁻², 1 × 10⁻², 2 × 10⁻³, and 1 × 10⁻³ diluted with DNase-free water). The negative-control samples contained DNase-free water instead of template DNA. To determine the initial concentrations, cells were counted using a Neubauer hemocytometer with a 0.01-mm depth (Marienfeld, Lauda-Knigshofen, Germany).

The amplification was carried out using the DyNamo Flash SYBR green qPCR kit (Biozyme, Hessisch Oldendorf, Germany) according to the manufacturer's instructions. The optimal annealing temperature was determined using a temperature gradient qPCR. All qPCRs were analyzed in a CFX96 cyler (Bio-Rad, Munich, Germany). The amplification was conducted using the following program: 5 min at 95°C for predenaturation and then 34 cycles of 10 s at 95°C for denaturation, 30 s at 56°C for annealing, and 30 s 60°C for extension reactions. As a last step, a melting curve from 60°C to 95°C was used to analyze the purity of the qPCR products. The amplified DNA samples were loaded on a 2.5% agarose gel for verification of the expected fragment length. The C_T values were automatically calculated with the Bio-Rad CFX Manager software. The standard curves were obtained by plotting the C_T values against the logarithm of the concentration of each dilution of template DNA. For *S. oneidensis* and *G. sulfurreducens*, primers described by Dolch et al. (29) were used. For *G. metallireducens*, specific primers were designed with the software tool Geneious (Biomatters, Auckland, New Zealand). All primer sequences are listed in Table 2.

Fluorescence *in situ* hybridization. FISH was used for the simultaneous visualization, identification, and localization of each strain in the multispecies biofilm community. Samples for FISH were taken from the planktonic phase and directly from the anode surface at the completion of the experiment. Liquid samples were fixed with 4% formaldehyde for 1 h at 4°C. Afterwards, they were washed twice in phosphate-buffered saline (PBS) [2.7 mM KCl, 1.76 mM KH₂PO₄, 137 mM NaCl, 10 mM Na₂HPO₄, 9 mM (NH₄)₂SO₄, 1 mM Mg₂SO₄, 0.1 mM CaCl₂, pH 7] via centrifuging at a relative centrifugal force (RCF) of 8,000 for 2 min. The samples were then stored in a 50% (vol/vol) ethanol solution at -20°C. Complete anodes were fixed with the same concentration of formaldehyde for 4 h at 4°C. Thereafter, they were washed in PBS for 30 min and then stored at 4°C. FISH analysis was conducted as described by Dolch et

TABLE 3 Fluorescently labeled oligonucleotide probes and helper oligonucleotides for FISH

Probe name	Sequence (5' to 3')	Specification	Reference
SHEW227	AGCTAATCCCACCTAGGTWCATC	<i>Shewanella</i> spp.	60
GEO1	AGAATCCAAGGACTCCGT	<i>G. metallireducens</i>	15
HGEO1-1	GAAGGTCCCCCTTTTCCCGC	Helpers for GEO1	— ^a
HGEO1-2	GGGCTTATCCGGTATTAGCACC	Helpers for GEO1	—
GEO2	AGAATCCAAGGACTCCGT	<i>G. sulfurreducens</i>	61
HGEO2-1	GTCCCCCTTTTCCCGCAAGA	Helpers for GEO2	61
HGEO2-2	CTAATGGTACGCGGACTCATCC	Helpers for GEO2	61

^a—, none.

al. (29) with the probes specified in Table 3. Images were collected with a Leica DM 5500 B microscope using a 63× immersion lens and a digital color camera (DFC 300 FX; Leica, Wetzlar, Germany). The filter sets used are listed in Table 4.

Single-nucleotide resolution RNA sequencing. RNA was extracted individually from the triplicates of four experimental BES setups, which were inoculated either with pure cultures of *S. oneidensis*, *G. sulfurreducens*, or *G. metallireducens* or with a coculture of the three strains. Prior to the extraction, all anodes with a biofilm were additionally preincubated in 3 ml of bacterial protection solution for 10 min at room temperature (RNeasy minikit; Qiagen, Hilden, Germany). Total RNA was isolated from the anode biofilms using the RNeasy kit provided by Qiagen according to the manufacturer's instructions. Residual DNA was removed with an overnight DNase I digestion at 37°C. Further purification of RNA from DNA was conducted using the Ambion DNA-free kit (Life Technologies, Carlsbad, CA, USA). Aliquots from treated samples were subjected to PCR amplification with specific primers (Table 2) to validate the absence of genomic DNA. The Ambion MICROBExpress bacterial mRNA enrichment kit (Life Technologies) was used for rRNA depletion. Strand-specific cDNA libraries were prepared from 50 ng of rRNA-depleted RNA following the TruSeq v2 RNA protocol (Illumina). The libraries were prepared using multiplex primers to enable simultaneous sequencing on a single lane, which was performed on a HiSeq1500 system using SBS v3 kits (Illumina), generating paired-end reads of 2 × 51 nucleotides (nt) (*G. sulfurreducens* and *S. oneidensis*) or 2 × 100 nt (coculture and *G. metallireducens* samples). Cluster detection and base calling were performed using RTAv1.13, and the quality of reads was assessed with CASAVA v1.8.1 (Illumina).

RNA-sequencing data analysis. Sequence data were clipped for the samples with 2 × 100 nt to obtain a fixed read length of 51 nt in all samples and were mapped to a database containing the merged genomes of *G. sulfurreducens* (NCBI GenBank accession number [NC_002939.5](#)), *G. metallireducens* ([NC_007517.1](#)), *S. oneidensis* ([NC_004347.2](#)), and its megaplasmid ([NC_004349.1](#)) using Bowtie (56). Differential expression profiles were calculated individually for each species in pure cultures versus the coculture by comparing the gene expression levels from the mapped sequences using HTSeq (57) for counting and DESeq2 (58) for differential expression analysis. An adjusted *P* value (*P* adj) of 0.05 was used as the threshold to determine statistical significance for differential gene expression.

Analytical techniques. Organic acids that were consumed or produced during the experiments were quantified using high-performance liquid chromatography (HPLC). Organic acids were quantified as described by Sturm-Richter et al. (59). Cell densities were determined via the Thermo Scientific GENESYS 20 spectrophotometer.

Oxygen measurements. Oxygen was detected with the fiber-optic oxygen meter Microx-TX3 and a needle-type housing oxygen microsensor according to the manufacturers' instructions (PreSens, Germany). For 2-point calibration, an anoxic 57.5 mM sodium dithionite solution and air-saturated water were used as minimum and maximum references for oxygen saturation, respectively. The anodic oxygen concentration was measured in each reactor at the completion of the experiments.

Flavin quantification. Liquid samples of the BES were collected at different time points. The samples were centrifuged (6,000 rpm, 5 min) and filtered through a 0.2-μm-pore-size filter. Samples 200 μl in volume were transferred to a UV-transparent microtiter plate and read in a Tecan Infinite M200 PRO plate reader (Tecan, Austria) at 440 nm excitation and 525 nm emission. Different concentrations ranging from 25 nM to 2.5 μM of a mixture of flavin mononucleotide (FMN) and riboflavin (80:20) were used for establishing a standard calibration curve.

Accession number(s). Single-nucleotide resolution RNA sequencing of cocultures and biofilms yielded between 2.3 and 37.2 million read pairs that have been deposited into the NCBI GEO database under the accession number [GSE79750](#).

TABLE 4 Specifications of the filters for FISH used in the Leica DM 5500 B microscope

Filter cube	Fluor dye	Excitation color	Excitation filter	Suppression filter
A4	DAPI ^a	UV	BP 360/40	BP 470/40
I3	FITC	Blue	BP 450/490	LP 515
Y3	CY3	Green	BP 545/30	BP 610/75
Y5	CY5	Red	BP 640/30	BP 690/50

^aDAPI, 4',6-diamidino-2-phenylindole.

SUPPLEMENTAL MATERIAL

Supplemental material for this article may be found at <https://doi.org/10.1128/AEM.03033-16>.

TEXT S1, PDF file, 0.07 MB.

DATA SET S1, XLSX file, 0.1 MB.

ACKNOWLEDGMENT

This research was supported by the German Ministry of Education and Research (BMBF) (03SF0424A).

REFERENCES

- Lovley DR, Coates JD, Blunt-Harris EL, Phillips EJP, Woodward JC. 1996. Humic substances as electron acceptors for microbial respiration. *Nature* 382:445–448. <https://doi.org/10.1038/382445a0>.
- Lovley DR, Holmes DE, Nevin KP. 2004. Dissimilatory Fe(III) and Mn(IV) reduction. *Adv Microb Physiol* 49:219–286. [https://doi.org/10.1016/S0065-2911\(04\)49005-5](https://doi.org/10.1016/S0065-2911(04)49005-5).
- Myers CR, Nealon KH. 1988. Bacterial manganese reduction and growth with manganese oxide as the sole electron acceptor. *Science* 240:1319–1321. <https://doi.org/10.1126/science.240.4857.1319>.
- Richter K, Schicklberger M, Gescher J. 2012. Dissimilatory reduction of extracellular electron acceptors in anaerobic respiration. *Appl Environ Microbiol* 78:913–921. <https://doi.org/10.1128/AEM.06803-11>.
- Straub KL, Benz M, Schink B. 2001. Iron metabolism in anoxic environments at near neutral pH. *FEMS Microbiol Ecol* 34:181–186. <https://doi.org/10.1111/j.1574-6941.2001.tb00768.x>.
- Logan BE. 2009. Exoelectrogenic bacteria that power microbial fuel cells. *Nat Rev Microbiol* 7:375–381. <https://doi.org/10.1038/nrmicro2113>.
- Logan BE, Regan JM. 2006. Electricity-producing bacterial communities in microbial fuel cells. *Trends Microbiol* 14:512–518. <https://doi.org/10.1016/j.tim.2006.10.003>.
- Sydow A, Krieg T, Mayer F, Schrader J, Holtmann D. 2014. Electroactive bacteria—molecular mechanisms and genetic tools. *Appl Microbiol Biotechnol* 98:8481–8495. <https://doi.org/10.1007/s00253-014-6005-z>.
- Chen X, Liang P, Zhang XY, Huang X. 2016. Bioelectrochemical systems-driven directional ion transport enables low-energy water desalination, pollutant removal, and resource recovery. *Bioresour Technol* 215:274–284. <https://doi.org/10.1016/j.biortech.2016.02.107>.
- Flynn JM, Ross DE, Hunt KA, Bond DR, Gralnick JA. 2010. Enabling unbalanced fermentations by using engineered electrode-interfaced bacteria. *mBio* 1:e00190-10. <https://doi.org/10.1128/mBio.00190-10>.
- Wang HM, Luo HP, Fallgren PH, Jin S, Ren ZJ. 2015. Bioelectrochemical system platform for sustainable environmental remediation and energy generation. *Biotechnol Adv* 33:317–334. <https://doi.org/10.1016/j.biotechadv.2015.04.003>.
- Ishii S, Suzuki S, Norden-Krichmar TM, Phan T, Wanger G, Nealon KH, Sekiguchi Y, Gorby YA, Bretschger O. 2014. Microbial population and functional dynamics associated with surface potential and carbon metabolism. *ISME J* 8:963–978. <https://doi.org/10.1038/ismej.2013.217>.
- Wang LY, Nevin KP, Woodard TL, Mu BZ, Lovley DR. 2016. Expanding the diet for DIET: electron donors supporting direct interspecies electron transfer (DIET) in defined co-cultures. *Front Microbiol* 7:236. <https://doi.org/10.3389/fmicb.2016.00236>.
- Dolfing J. 2014. Syntrophy in microbial fuel cells. *ISME J* 8:4–5. <https://doi.org/10.1038/ismej.2013.198>.
- Summers ZM, Fogarty HE, Leang C, Franks AE, Malvankar NS, Lovley DR. 2010. Direct exchange of electrons within aggregates of an evolved syntrophic coculture of anaerobic bacteria. *Science* 330:1413–1415. <https://doi.org/10.1126/science.1196526>.
- Read ST, Dutta P, Bond PL, Keller J, Rabaey K. 2010. Initial development and structure of biofilms on microbial fuel cell anodes. *BMC Microbiol* 10:98. <https://doi.org/10.1186/1471-2180-10-98>.
- Venkataraman A, Rosenbaum MA, Perkins SD, Werner JJ, Angenent LT. 2011. Metabolite-based mutualism between *Pseudomonas aeruginosa* PA14 and *Enterobacter aerogenes* enhances current generation in bioelectrochemical systems. *Energy Environ Sci* 4:4550–4559. <https://doi.org/10.1039/c1ee01377g>.
- Rosenbaum MA, Bar HY, Beg QK, Segre D, Booth J, Cotta MA, Angenent LT. 2011. *Shewanella oneidensis* in a lactate-fed pure-culture and a glucose-fed co-culture with *Lactococcus lactis* with an electrode as electron acceptor. *Bioresour Technol* 102:2623–2628. <https://doi.org/10.1016/j.biortech.2010.10.033>.
- Sturm G, Dolch K, Richter K, Rautenberg M, Gescher J. 2012. Metal reducers and reduction targets. A short survey about the distribution of dissimilatory metal reducers and the multitude of terminal electron acceptors, p 129–159. *In* Gescher J, Kappler A (ed), *Microbial metal respiration: from geochemistry to potential applications*. Springer, Berlin, Germany.
- Wagner RC, Call DI, Logan BE. 2010. Optimal set anode potentials vary in bioelectrochemical systems. *Environ Sci Technol* 44:6036–6041. <https://doi.org/10.1021/es101013e>.
- Aelterman P, Freguia S, Keller J, Verstraete W, Rabaey K. 2008. The anode potential regulates bacterial activity in microbial fuel cells. *Appl Microbiol Biotechnol* 78:409–418. <https://doi.org/10.1007/s00253-007-1327-8>.
- Ishii S, Suzuki S, Norden-Krichmar TM, Wu A, Yamanaka Y, Nealon KH, Bretschger O. 2013. Identifying the microbial communities and operational conditions for optimized wastewater treatment in microbial fuel cells. *Water Res* 47:7120–7130. <https://doi.org/10.1016/j.watres.2013.07.048>.
- Scott JH, Nealon KH. 1994. A biochemical study of the intermediary carbon metabolism of *Shewanella putrefaciens*. *J Bacteriol* 176:3408–3411. <https://doi.org/10.1128/jb.176.11.3408-3411.1994>.
- Venkateswaran K, Moser DP, Dollhopf ME, Lies DP, Saffarini DA, MacGregor BJ, Ringelberg DB, White DC, Nishijima M, Sano H, Burghardt J, Stackebrandt E, Nealon KH. 1999. Polyphasic taxonomy of the genus *Shewanella* and description of *Shewanella oneidensis* sp. nov. *Int J Syst Bacteriol* 49:705–724. <https://doi.org/10.1099/00207713-49-2-705>.
- von Canstein H, Ogawa J, Shimizu S, Lloyd JR. 2008. Secretion of flavins by *Shewanella* species and their role in extracellular electron transfer. *Appl Environ Microbiol* 74:615–623. <https://doi.org/10.1128/AEM.01387-07>.
- Marsili E, Baron DB, Shikhare ID, Coursolle D, Gralnick JA, Bond DR. 2008. *Shewanella* secretes flavins that mediate extracellular electron transfer. *Proc Natl Acad Sci U S A* 105:3968–3973. <https://doi.org/10.1073/pnas.0710525105>.
- Kotloski NJ, Gralnick JA. 2013. Flavin electron shuttles dominate extracellular electron transfer by *Shewanella oneidensis*. *mBio* 4:e00553-12. <https://doi.org/10.1128/mBio.00553-12>.
- Lanthier M, Gregory KB, Lovley DR. 2008. Growth with high planktonic biomass in *Shewanella oneidensis* fuel cells. *FEMS Microbiol Lett* 278:29–35. <https://doi.org/10.1111/j.1574-6968.2007.00964.x>.
- Dolch K, Danzer J, Kabbeck T, Bierer B, Erben J, Forster AH, Maisch J, Nick P, Kerzenmacher S, Gescher J. 2014. Characterization of microbial current production as a function of microbe-electrode-interaction. *Bioresour Technol* 157:284–292. <https://doi.org/10.1016/j.biortech.2014.01.112>.
- Caccavo F, Lonergan DJ, Lovley DR, Davis M, Stolz JF, McInerney MJ. 1994. *Geobacter sulfurreducens* sp. nov., a hydrogen- and acetate-oxidizing dissimilatory metal-reducing microorganism. *Appl Environ Microbiol* 60:3752–3759.
- Lin WC, Coppi MV, Lovley DR. 2004. *Geobacter sulfurreducens* can grow with oxygen as a terminal electron acceptor. *Appl Environ Microbiol* 70:2525–2528. <https://doi.org/10.1128/AEM.70.4.2525-2528.2004>.
- Lovley DR, Phillips EJP. 1988. Novel mode of microbial energy metabolism: organic carbon oxidation coupled to dissimilatory reduction of iron or manganese. *Appl Environ Microbiol* 54:1472–1480.
- Rotaru AE, Woodard TL, Nevin KP, Lovley DR. 2015. Link between capacity

- for current production and syntrophic growth in *Geobacter* species. *Front Microbiol* 6:744. <https://doi.org/10.3389/fmicb.2015.00744>.
34. Lovley DR, Giovannoni SJ, White DC, Champine JE, Phillips EJP, Gorby YA, Goodwin S. 1993. *Geobacter metallireducens* gen. nov. sp. nov., a microorganism capable of coupling the complete oxidation of organic compounds to the reduction of iron and other metals. *Arch Microbiol* 159:336–344. <https://doi.org/10.1007/BF00290916>.
 35. Tan Y, Adhikari RY, Malvankar NS, Ward JE, Nevin KP, Woodard TL, Smith JA, Snoeyenbos-West OL, Franks AE, Tuominen MT, Lovley DR. 2016. The low conductivity of *Geobacter uranireducens* pili suggests a diversity of extracellular electron transfer mechanisms in the genus *Geobacter*. *Front Microbiol* 7:980. <https://doi.org/10.3389/fmicb.2016.00980>.
 36. Brutinel ED, Gralnick JA. 2012. Shuttling happens: soluble flavin mediators of extracellular electron transfer in *Shewanella*. *Appl Microbiol Biotechnol* 93:41–48. <https://doi.org/10.1007/s00253-011-3653-0>.
 37. Ross DE, Brantley SL, Tien M. 2009. Kinetic characterization of OmcA and MtrC, terminal reductases involved in respiratory electron transfer for dissimilatory iron reduction in *Shewanella oneidensis* MR-1. *Appl Environ Microbiol* 75:5218–5226. <https://doi.org/10.1128/AEM.00544-09>.
 38. Summers ZM, Ueki T, Ismail W, Haveman SA, Lovley DR. 2012. Laboratory evolution of *Geobacter sulfurreducens* for enhanced growth on lactate via a single-base-pair substitution in a transcriptional regulator. *ISME J* 6:975–983. <https://doi.org/10.1038/ismej.2011.166>.
 39. Ueki T, Lovley DR. 2010. Genome-wide gene regulation of biosynthesis and energy generation by a novel transcriptional repressor in *Geobacter* species. *Nucleic Acids Res* 38:810–821. <https://doi.org/10.1093/nar/gkp1085>.
 40. Coppi MV, O'Neil RA, Lovley DR. 2004. Identification of an uptake hydrogenase required for hydrogen-dependent reduction of Fe(III) and other electron acceptors by *Geobacter sulfurreducens*. *J Bacteriol* 186:3022–3028. <https://doi.org/10.1128/JB.186.10.3022-3028.2004>.
 41. Giuffrè A, Borisov VB, Aresè M, Sarti P, Forte E. 2014. Cytochrome *bd* oxidase and bacterial tolerance to oxidative and nitrosative stress. *Biochim Biophys Acta* 1837:1178–1187. <https://doi.org/10.1016/j.bbabi.2014.01.016>.
 42. Akhujkar M, Krushkal J, DiBartolo G, Lapidus A, Land ML, Lovley DR. 2009. The genome sequence of *Geobacter metallireducens*: features of metabolism, physiology and regulation common and dissimilar to *Geobacter sulfurreducens*. *BMC Microbiol* 9:109. <https://doi.org/10.1186/1471-2180-9-109>.
 43. Suvorova IA, Ravcheev DA, Gelfand MS. 2012. Regulation and evolution of malonate and propionate catabolism in proteobacteria. *J Bacteriol* 194:3234–3240. <https://doi.org/10.1128/JB.00163-12>.
 44. Salmond CV, Kroll RG, Booth IR. 1984. The effect of food preservatives on pH homeostasis in *Escherichia coli*. *J Gen Microbiol* 130:2845–2850.
 45. Horswill AR, Dudding AR, Escalante-Semerena JC. 2001. Studies of propionate toxicity in *Salmonella enterica* identify 2-methylcitrate as a potent inhibitor of cell growth. *J Biol Chem* 276:19094–19101. <https://doi.org/10.1074/jbc.M100244200>.
 46. Meshulam-Simon G, Behrens S, Choo AD, Spormann AM. 2007. Hydrogen metabolism in *Shewanella oneidensis* MR-1. *Appl Environ Microbiol* 73:1153–1165. <https://doi.org/10.1128/AEM.01588-06>.
 47. Kazakov AE, Rodionov DA, Alm E, Arkin AP, Dubchak I, Gelfand MS. 2009. Comparative genomics of regulation of fatty acid and branched-chain amino acid utilization in proteobacteria. *J Bacteriol* 191:52–64. <https://doi.org/10.1128/JB.01175-08>.
 48. Dunny GM, Brickman TJ, Dworkin M. 2008. Multicellular behavior in bacteria: communication, cooperation, competition and cheating. *Bioessays* 30:296–298. <https://doi.org/10.1002/bies.20740>.
 49. Czarán T, Hoekstra RF. 2010. Microbial communication, cooperation and cheating: quorum sensing drives the evolution of cooperation in bacteria. *Virulence* 1:402–403. <https://doi.org/10.4161/viru.1.5.12549>.
 50. Coppi MV, Leang C, Sandler SJ, Lovley DR. 2001. Development of a genetic system for *Geobacter sulfurreducens*. *Appl Environ Microbiol* 67:3180–3187. <https://doi.org/10.1128/AEM.67.7.3180-3187.2001>.
 51. Holmes DE, Bond DR, Lovley DR. 2004. Electron transfer by *Desulfobulbus propionicus* to Fe(III) and graphite electrodes. *Appl Environ Microbiol* 70:1234–1237. <https://doi.org/10.1128/AEM.70.2.1234-1237.2004>.
 52. Straub KL, Schink B. 2004. Ferrihydrite reduction by *Geobacter* species is stimulated by secondary bacteria. *Arch Microbiol* 182:175–181. <https://doi.org/10.1007/s00203-004-0686-0>.
 53. Balch WE, Wolfe RS. 1976. New approach to cultivation of methanogenic bacteria: 2-mercaptoethanesulfonic acid (HS-CoM)-dependent growth of *Methanobacterium ruminantium* in a pressurized atmosphere. *Appl Environ Microbiol* 32:781–791.
 54. Kloke A, Rubenwolf S, Buecking C, Gescher J, Kerzenmacher S, Zengerle R, von Stetten F. 2010. A versatile miniature bioreactor and its application to bioelectrochemistry studies. *Biosens Bioelectron* 25:2559–2565. <https://doi.org/10.1016/j.bios.2010.04.014>.
 55. Dolch K, Wuske J, Gescher J. 2016. Genomic barcode-based analysis of exoelectrogens in wastewater biofilms grown on anode surfaces. *J Microbiol Biotechnol* 26:511–520. <https://doi.org/10.4014/jmb.1510.10102>.
 56. Langmead B, Salzberg SL. 2012. Fast gapped-read alignment with Bowtie 2. *Nat Methods* 9:357–359. <https://doi.org/10.1038/nmeth.1923>.
 57. Anders S, Huber W. 2010. Differential expression analysis for sequence count data. *Genome Biol* 11:R106. <https://doi.org/10.1186/gb-2010-11-10-r106>.
 58. Love MI, Huber W, Anders S. 2014. Moderated estimation of fold change and dispersion for RNA-seq data with DESeq2. *Genome Biol* 15:550. <https://doi.org/10.1186/s13059-014-0550-8>.
 59. Sturm-Richter K, Golitsch F, Sturm G, Kipf E, Dittrich A, Beblawy S, Kerzenmacher S, Gescher J. 2015. Unbalanced fermentation of glycerol in *Escherichia coli* via heterologous production of an electron transport chain and electrode interaction in microbial electrochemical cells. *Bioreour Technol* 186:89–96. <https://doi.org/10.1016/j.biortech.2015.02.116>.
 60. Huggett MJ, Crocetti GR, Kjelleberg S, Steinberg PD. 2008. Recruitment of the sea urchin *Heliocidaris erythrogramma* and the distribution and abundance of inducing bacteria in the field. *Aquat Microb Ecol* 53:161–171. <https://doi.org/10.3354/ame01239>.
 61. Richter HLM, Nevin KP, Lovley DR. 2007. Lack of electricity production by *Pelobacter carbinolicus* indicates that the capacity for Fe(III) oxide reduction does not necessarily confer electron transfer ability to fuel cell anodes. *Appl Environ Microbiol* 73:5347–5353. <https://doi.org/10.1128/AEM.00804-07>.